Response to reviewer #1

We thank the reviewer for those supportive and thoughtful comments. Our responses to the comments are provided below in blue, with the reviewers' comments in black.

General Comments:

In this study, a combined DMA-CPMA-CPC system was applied to characterize the size-resolved particle effective density in Multiphase chemistry experiment in Fogs and Aerosols in the North China Plain (McFAN) in autumn 2019. They identified a frequent bimodal distribution of particle effective density, and a unique low-density mode (named sub-density mode) accounted for ~20-30% of total observed particles. The diurnal variations of particle effective density and the influence of pollution and secondary aerosols were discussed. They concluded that the influence of BC on the effective density is even stronger than SIA.

Overall, the paper is well-written and is appropriate for ACP. The results clearly indicate the factors that govern the variations of particle effective density. The size-resolved particle effective density shown in the manuscript is interesting and would have implications for further studies. Some minor comments are still needed to be addressed before the manuscript can be published.

Response:

Thank you for the positive feedback and helpful suggestions. We have addressed the comments and implemented all suggestions in the revised manuscript as detailed below.

Specific Comments

1. The authors directly linked the sub-density mode to fresh black carbon (BC) emissions. Some organics might also have very low densities, which might lead to ambiguous conclusions. Previous measurements have also indicated that organics dominated in smaller size ranges. This is a key requirement when clarify the significance of BC in such mode.

Response:

Thanks for the comment. We agree with the reviewer that some organics might have very low densities and contribute to the sub-density mode. Therefore, we tried to assess the possible contribution of BC and organics on the sub-density mode via the correlation analysis between the number fraction of the sub-density mode (F_{sub}) and the mass fractions of BC and organics in PM_1. Unfortunately, there was no measurement of the chemical composition of ultrafine particles (diameter < 100 nm) during our experiment and we could not determine the actual contribution of organics in the sub-density mode at 50 and 100 nm. Accordingly, we have added this discussion in Sect. 3.1 as: "*On the other hand, a low effective density mode (density < 1.20 g cm^{-3}) exists or even dominates in the measurements near emission sources, which is ascribed to freshly emitted particles and non-uniformly mixed particles (Nosko and Olofsson, 2017; Olfert and Rogak, 2019; Park et al., 2003). Numerous studies have found low effective densities of freshly emitted BC, with a minimum of 0.10 g cm^{-3} (Pagels et al., 2009). While the density of OA is usually assumed as 1.2-1.3 g cm^{-3} in most cases (Hallquist et al., 2009), some studies have found it could be as low as 0.6-1.1 g cm^{-3} (Nakao et al.,*

2011; Li et al., 2016). To eluciate the role of these two components in the sub-density mode, we further analyze the correlation between the number fraction of the sub-density mode (F_{sub}) and the mass fractions of BC and OA. As seen in Fig. S6-S7, the mass fraction of BC shows significant correlation with F_{sub} at 150, 220 and 300 nm (R^2 = 0.46-0.57), whereas barely no correlation is observed between OA and F_{sub} (R^2 = 0.02-0.09), implying that the sub-density mode at these three sizes could be mainly attributed to freshly emitted BC and the quantity of the sub-density mode is closely related to the variation of BC mass fraction. However, F_{sub} at 50-100 nm shows little correlation with either BC or OA mass fraction, which could be explained by the difference between the PM_1 bulk chemical composition and the chemical composition of particles smalller than 100 nm."

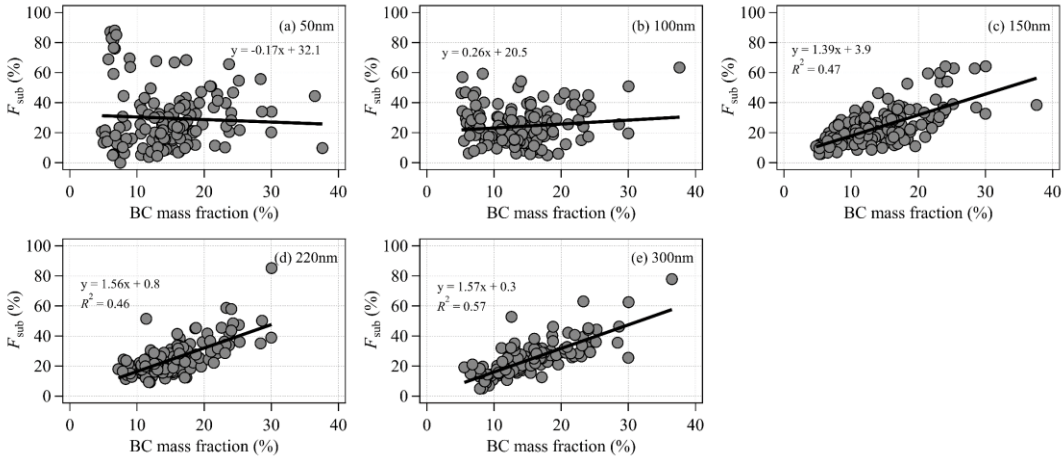

Figure R1 (S6). Correlation between BC mass fraction and the number fraction of the sub-density mode (F_{sub}) for (a) 50 nm, (b) 100 nm, (c) 150 nm, (d) 220 nm, and (e) 300 nm particles.

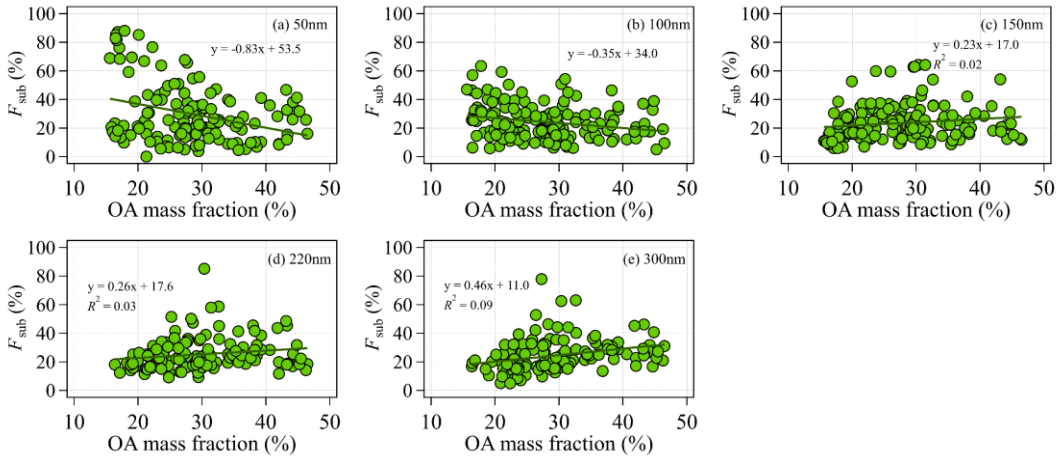

Figure R2 (S7). Correlation between OA mass fraction and the number fraction of the sub-density mode (F_{sub}) for (a) 50 nm, (b) 100 nm, (c) 150 nm, (d) 220 nm, and (e) 300 nm particles.

2. It would be better to include uncertainty data when expressing the mean density in the abstract.

Response:

Thanks for the suggestion. Following the reviewer's suggestion, we have added the standard deviation of the entire measurement when expressing the measured values in the abstract as: "*The geometric mean for the main-density mode ($\bar{\rho}_{eff,main}$) increases from 1.18±0.10 g cm^{-3} (50 nm) to 1.37±0.12 g cm^{-3} (300 nm) due to larger fraction of high-density components and more significant restructuring effect at large particle sizes, but decreases from 0.89±0.08 g cm^{-3} (50 nm) to 0.62±0.12 g cm^{-3} (300 nm) for the sub-density mode ($\bar{\rho}_{eff,sub}$) which could be mainly ascribed to the agglomerate effect of BC.*"

3. abstract: "…for the sub-density mode ($\bar{\rho}_{\mathrm{eff,sub}}$) ascribed to the agglomerate effect." Does it refer to the agglomerate effect of BC?

Response:

Yes, it refers to the agglomerate effect of BC. To make it clear, the sentence has been revised as "*…but decreases from 0.89±0.08 g cm^{-3} (50 nm) to 0.62±0.12 g cm^{-3} (300 nm) for the sub-density mode ($\bar{\rho}_{eff,sub}$) which could be mainly ascribed to the agglomerate effect of BC.*"

4. Line 113: "A combined DMA-CPMA-CPC system was employed to measure the size-resolved effective density of particles with mobility diameter of 50, 100, 150, 220, and 300 nm" what is the uncertainty for the size selection?

Response:

Thanks for the comment. The sizing uncertainty of DMA and the overall measurement uncertainty of the DMA-CPMA-CPC system were evaluated using polystyrene latex (PSL) particles. A description of the uncertainties has been added in Sect. 2.1 as: "*The measurement uncertainty of the DMA-CPMA-CPC system could come from two aspects: the size classification of DMA and the mass classification of CPMA. Based on the test using polystyrene latex (PSL) particles with diameters of 150, 220, and 300 nm, an average sizing uncertainty of ±2 % was determined for our DMA (Fig. S4). This uncertainty is similar to the value of ±1 % (±1 nm) reported by Mulholland et al. (1999) for the size range of 100-300 nm at an aerosol-sheath flow rate ratio of 0.1. The uncertainty of the mass classification of CPMA is estimated as 1.4 % according to the results of Taylor and Kuyatt (1994) and Symonds et al. (2013). The overall measurement uncertainty of the DMA-CPMA-CPC system were also evaluated using PSL particles with diameter of 150, 220, and 300 nm before and after the field campaign. An uncertainty within ~ 5 % was found by comparing the measured effective densities with PSL material density (1.05 g cm^{-3}) (Fig. S5).*"

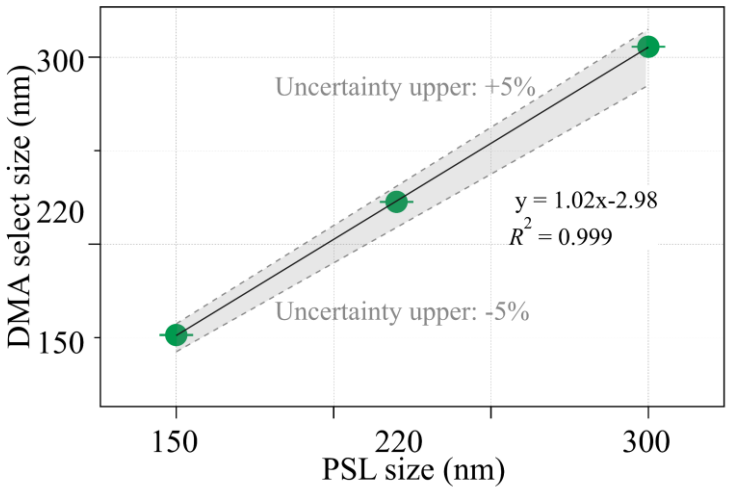

Figure R3 (S4). Uncertainty of DMA size selection.

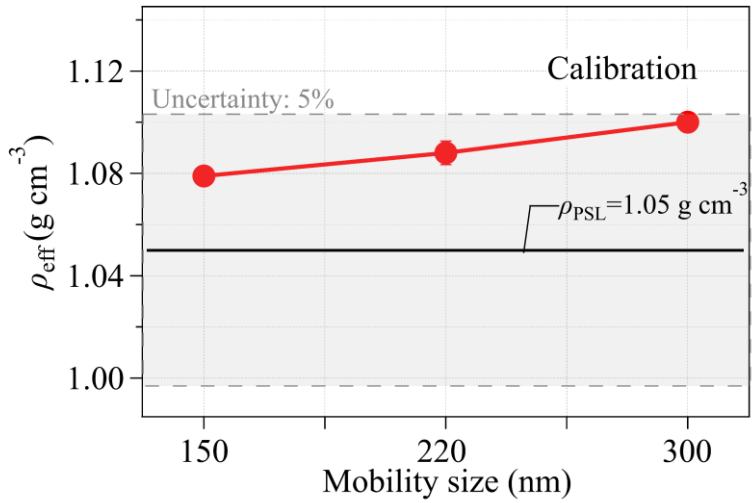

Figure R4 (S5). Calibration results for DMA-CPMA-CPC system.

5. Line 142-: It is necessary to show the uncertainty during the peak fitting with a flexible Gaussian fit algorithm, and thus potential contribution to the overall uncertainties.

Response:

Thanks for the comment. The reviewer suggested an important point for evaluating the performance of flexible Gaussian fit algorithm. We have evaluated the uncertainty of the flexible Gaussian fit algorithm and added a description in Sect. 2.2 as: "*The uncertainty of each individual Gaussian fit could be estimated based on the variation of the fitted* $\bar{\rho}_{eff,i}$ *in each mode at the 95 % confidence level. And the overall uncertainty is estimated by averaging the uncertainties of all the fits, which gives averages within 2.5 % and 7.0 % for* $\bar{\rho}_{eff,main}$ *and* $\bar{\rho}_{eff,sub}$ *at the five measured sizes, respectively. This uncertainty range is similar to the measurement uncertainty discussed in Sect. 2.1.*"

6. Line 205-: “The remarkably high occurrence of the sub-density mode in our study indicates a frequent influence of local BC emission.” Can these sub-density mode be matched to the variations of BC concentration?

Response:

Yes, this could be inferred by the well correlation between the area fractions of the sub-density mode (F_{sub}) with the BC mass fraction in PM_1 (Fig. R1). As raised in Comment #1 about the possible contribution of organics to the sub-density mode, we have now revised the corresponding paragraph to include the discussion about the role of BC and organics in the sub-density mode by performing correlation analysis between F_{sub} and the mass fractions of BC and OA in PM_1. Please see details in the response to Comment #1.

7. Line 309: “It indicates that photochemical aging process is very efficient in transiting particles from fractal to compact morphology.” In my opinion, the conclusion can only be obtained when the pollution during daytime and nighttime is at the same level. As discussed in the previous section, the pollution level over the study is highly varied, and thus the authors should compare the increase rate of Df under the similar conditions.

Response:

We thank the reviewer for the comment. We have now also estimated the increase rate of D_f under different pollution levels (categorized by $PM_{0.7}$ volume concentration) to minimize the influence of pollution level on the transiting particles from fractal to compact morphology. As shown in Fig. R5 (added as Fig.S16 in SI), a higher D_f increase rate at noon compared with night-time was observed at both the more polluted and the less polluted levels (Table R1, added as Table 3 in the revised manuscript), implying that photochemical aging process is very efficient in transiting particles from fractal to compact morphology.

The detailed discussion about the increase rate of D_f under different pollution levels has been added in Sect. 3.4 as: “*It is worth noting that the increase rate of D_f differs between noon and night, being ~0.12 h^{-1} at noon which is twice of the night-time increase rate (0.06 h^{-1}). To minimize the influence of pollution level on the transiting particles from fractal to compact morphology, the variation of D_f under the more polluted and the less polluted periods was further examined separately. As shown in Fig. S16, similar diurnal variations were observed at two different pollution levels, with a higher D_f increase rate at noon than night-time (Table 3), implying that photochemical aging process at noon is very efficient in transiting particles from fractal to compact morphology. It should be pointed out that there is no D_f data during 12:00-17:00 under the more polluted condition, likely due to the transition of the sub-density mode particles to the main-density mode associated with active aging processes. Given that D_f of the more polluted period is consistently 0.20 higher than the less polluted condition (Fig. S16) and aerosol aging process at noon is very active, the D_f increase rate from 11:00 to 13:00 under the more polluted condition is calculated by assuming a D_f of 3.0 at 13:00.*”

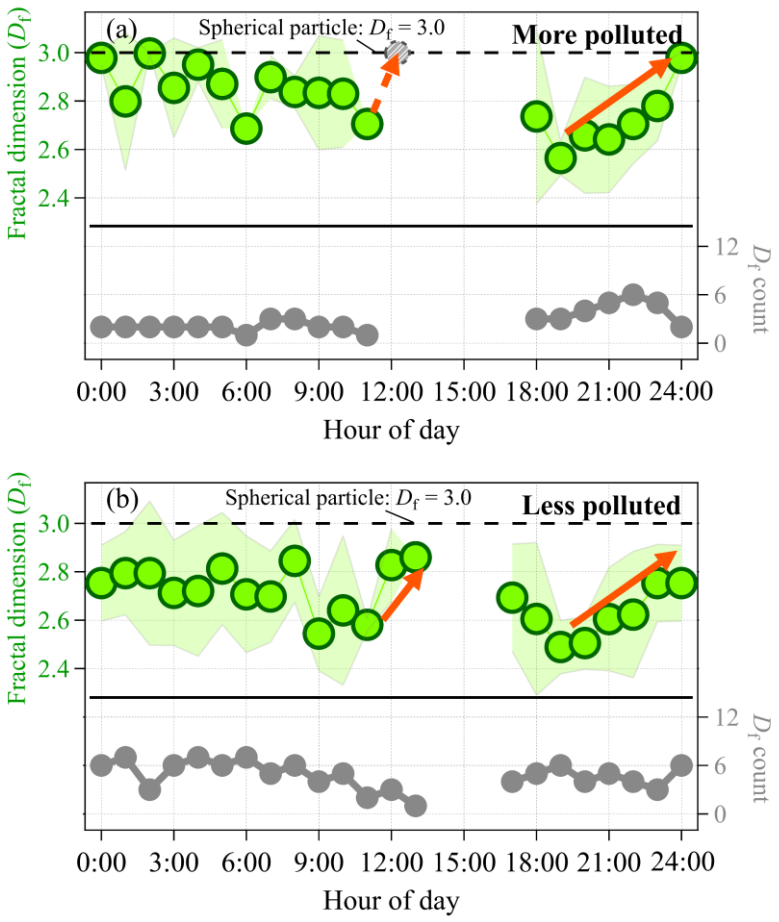

Figure R5 (S16). Diurnal cycle of fractal dimension (D_f) of the sub-density mode particles and D_f count under (a) the more and (b) the less polluted conditions. The dotted line is D_f with the value of 3.0, indicating particle with a spherical morphology. The orange arrows represent D_f with increasing trend. The grey dotted circle in the top figure represents the assumption of D_f = 3.0 at 13:00.

Table R1 (3). Comparison of fractal dimension (D_f) of the sub-density mode particles at noon and at night under the more and the less polluted conditions.

	D_f at 11:00	D_f at 13:00	Increase rate (h^{-1})	D_f at 19:00	D_f at 24:00	Increase rate (h^{-1})
All	2.62	2.86	0.12	2.51	2.80	0.06
More polluted	2.71	—	0.145*	2.56	2.98	0.08
Less polluted	2.58	2.86	0.14	2.49	2.75	0.05

* is calculated by assuming D_f at 13:00 is 3.0.

8. Section 4.4: Is it possible to assume a diurnal variation of BC density for the test in Figure 6, according to the source's strength of BC?

Response:

The source strength of BC exhibits not only diurnal cycle but also day-to-day variations. In the absence of detailed information on local emissions of BC and possible contribution from regional/long-range transport, it is quite difficult to directly assume a diurnal variation of BC effective density that accounts for the combination effects of different BC sources. Therefore, we tried an alternative method in which the BC effective density is retrieved for every three-hour of the day. The retrieved BC effective density does show some diurnal variation. However, due to the relatively small range of the diurnal variation as well as the marginal effect of the diurnal cycle on the correlation between $\bar{\rho}_{\mathrm{eff,tot,300nm}}$ and $\rho_{\mathrm{eff,ACSM}}$, we still adopt a fixed BC effective density of 0.60 g cm^{-3} for the $\rho_{\mathrm{eff,ACSM}}$ calculation in the revised manuscript.

We have thus added the corresponding discussion (also Fig. S18 and Fig. S19) about the diurnal variation of BC density in Sect. 3.5 as: "*Since strong diurnal variation was observed for BC mass fraction (Fig. S14) driven by the changes in primary source emissions, we also conduct a sensitivity analysis to retrieve BC effective density for every 3-hour of the day. The retrieved BC effective density indeed shows a diurnal pattern (Fig. S18), with high values in the afternoon and night and relatively low values during the morning and evening, which matches well with the diurnal pattern of* F_{sub} *(Fig. 5). However, the range of the diurnal variation (0.52-0.64 g cm*$^{-3}$*) is relatively small. When applying this diurnal pattern of BC effective density in the calculation of* $\rho_{eff,ACSM}$*, only a marginal increase was found in the* R^2 *of the correlation between* $\bar{\rho}_{eff,tot,300nm}$ *and* $\rho_{eff,ACSM}$ *(*R^2 *increased from 0.62 to 0.65, Fig. S19), probably due to the limited amount of data in each time interval and the use of bulk chemical composition in the calculation. Therefore, a fixed BC effective density of 0.60 g cm*$^{-3}$ *is used for the* $\rho_{eff,ACSM}$ *calculation in the following analysis.*"

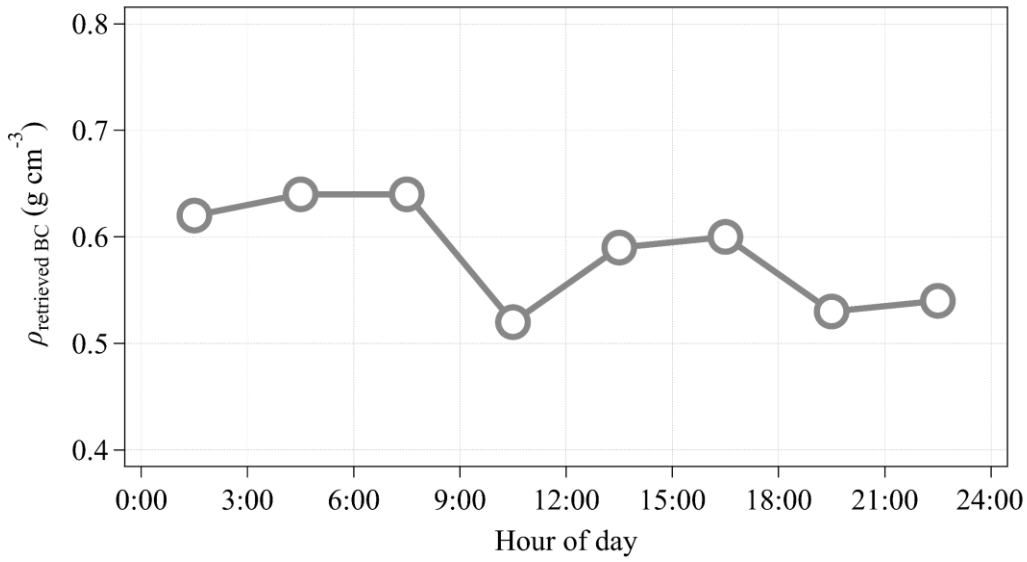

Figure R6 (S18). Diurnal variation of retrieved BC effective density.

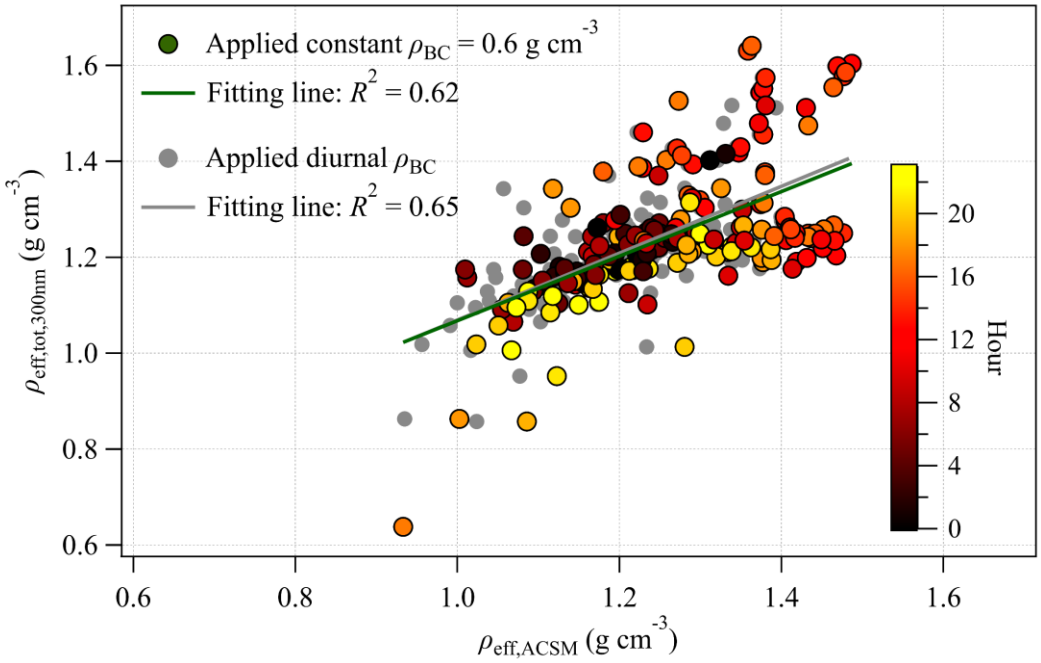

Figure R7 (S19). Comparison of the average effective density of particles at 300 nm observed by DMA-CPMA-CPC ($\bar{\rho}_{eff,tot,300nm}$) and ACSM-derived bulk effective density ($\rho_{eff,ACSM}$) by applied a constant ρ_{BC} or diurnal varied ρ_{BC}.

9. The conclusions should be shortened to be more concise, in particular, there are several numbers that are not really important.

Response:

Thanks for the comment. We have shortened and refined the conclusion in the revised manuscript.

Response to reviewer #2

We thank the reviewer for those supportive and thoughtful comments. Our responses to the comments are provided below in blue, with the reviewers' comments in black.

Dear Zhou et al.,

thank you for the interesting study regarding effective densities of ambient aerosol particles. The manuscript "Bimodal distribution of size-resolved particle effective density in a rural environment in the North China Plain" has been written very well and it is based on experiments conducted with state-of-the-art methods. The study presented in the manuscript aims to describe the effective density of ambient particles but also link it to the sources of particles, especially in case of observation of low effective densities. The figures of the manuscript are clear and mostly very informative and tables serve very well the structure of the manuscript.

Response:

We appreciated referee#2's positive feedback and constructive suggestions which are of great value for improving the quality of our paper. Our point-to-point replies to the referee's comments are listed below.

1. One relatively important issue in the presented study is the duration of the measurement campaign. I think the experimental period is not long enough to generalize the results. Regarding to that, is it possible to modify the title and abstract so that this is brought out to readers already in the beginning of the paper? Mentioning that the study is "case study" or "short campaign" would be enough for that purpose.

Response:

Thanks for the comment. We have changed the title to "*Bimodal distribution of size-resolved particle effective density**: results from a short campaign** in a rural environment in the North China Plain*" in the revised manuscript. We also revised the abstract accordingly: "*In this study, size-resolved particle effective density was measured with a combined DMA-CPMA-CPC system **in autumn 2019 as part of the** Multiphase chemistry experiment in Fogs and Aerosols in the North China Plain (McFAN).*"

2. As we all know, weather conditions have crucial role in aerosol formation, emission transportation and emission ageing, and they affect the ambient concentrations significantly. I propose that the authors include much more detailed weather data to the paper and investigate how the weather affect the effective densities of the particles. I think the affiliations of the authors enable the access to local weather data if it was not measured directly at particle measurement site. In addition, inclusion of the weather data into the paper enables better comparisons to other studies made later in same place or in other places by other researchers.

Response:

Thanks for this very constructive suggestion. We have now included the weather data (including wind speed, wind direction, relative humidity and temperature) measured at a standard weather station ~200 m away from the measurement container in the revised

manuscript. The overall weather condition is added to the timeseries plot (Fig. R1, added as Fig. S2 in SI). Accordingly, we have added one additional section (Sect. 3.2) as well as Fig. R2 (Fig. 3 in the revised manuscript) and Fig. R3-R4 (Fig. S10-S11 in SI) to specifically discuss the influence of meteorological conditions on both the pollution level and particle effective density:

"***3.2 Evolutions of effective density with meteorology conditions***

Weather conditions play a crucial role in the formation, aging and emission transportation of aerosol, and may therefore affect the distribution, composition, mixing state and consequently also the effective density of ambient aerosol. As seen in Fig. S2, the pollution level at the sampling site is sensitive to the variations of wind speed and direction during the observation period. Low $PM_{0.7}$ concentrations were usually presented with strong northerly winds while high $PM_{0.7}$ concentrations were associated with calm winds or southwest winds.

Figure 3 and Fig. S10 shows the average $\bar{\rho}_{eff,main}$, $\bar{\rho}_{eff,sub}$ and F_{sub} at each specific wind speed and direction. Obvious high values of $\bar{\rho}_{eff,main}$ and $\bar{\rho}_{eff,sub}$ appear with wind direction of southwest and wind speed > 2 m s^{-1}. This pattern clearly indicates the influence of regional transport from southern Hebei Province, an area greatly affected by emissions from industrial and residentials sources (Huang et al., 2019; Li et al., 2017). Air masses from this direction may bring pollutants with sufficient aging process, leading to changes in particle chemical composition and morphology, and consequently an increase in the fraction of particles closer to spherical with higher effective densities. Accordingly, F_{sub} also shows distinctly low values (Fig. 3c and Fig. S10). It is worth mentioning that $\bar{\rho}_{eff,main}$ and $\bar{\rho}_{eff,sub}$ do not show any obvious difference for wind direction of northwest. This implies that the influence of the traffic emission at No.107 National Way, which is approximate 1.5 km away from the sampling site (Fig. S1), on our measurements is somehow limited. We also noticed that an increasing trend of $\bar{\rho}_{eff,main}$ is presented with increasing wind speed (Fig. S11). This increase could be interpreted by the antagonism between well-aged particles from long-range transport and fresh particles from local emissions. High wind speed is usually accompanied with the long-range transport of particles with sufficient aging and consequently high effective density; while low wind speed generally implies higher contribution of local fresh emissions, resulting in more particles with non-spherical morphology."

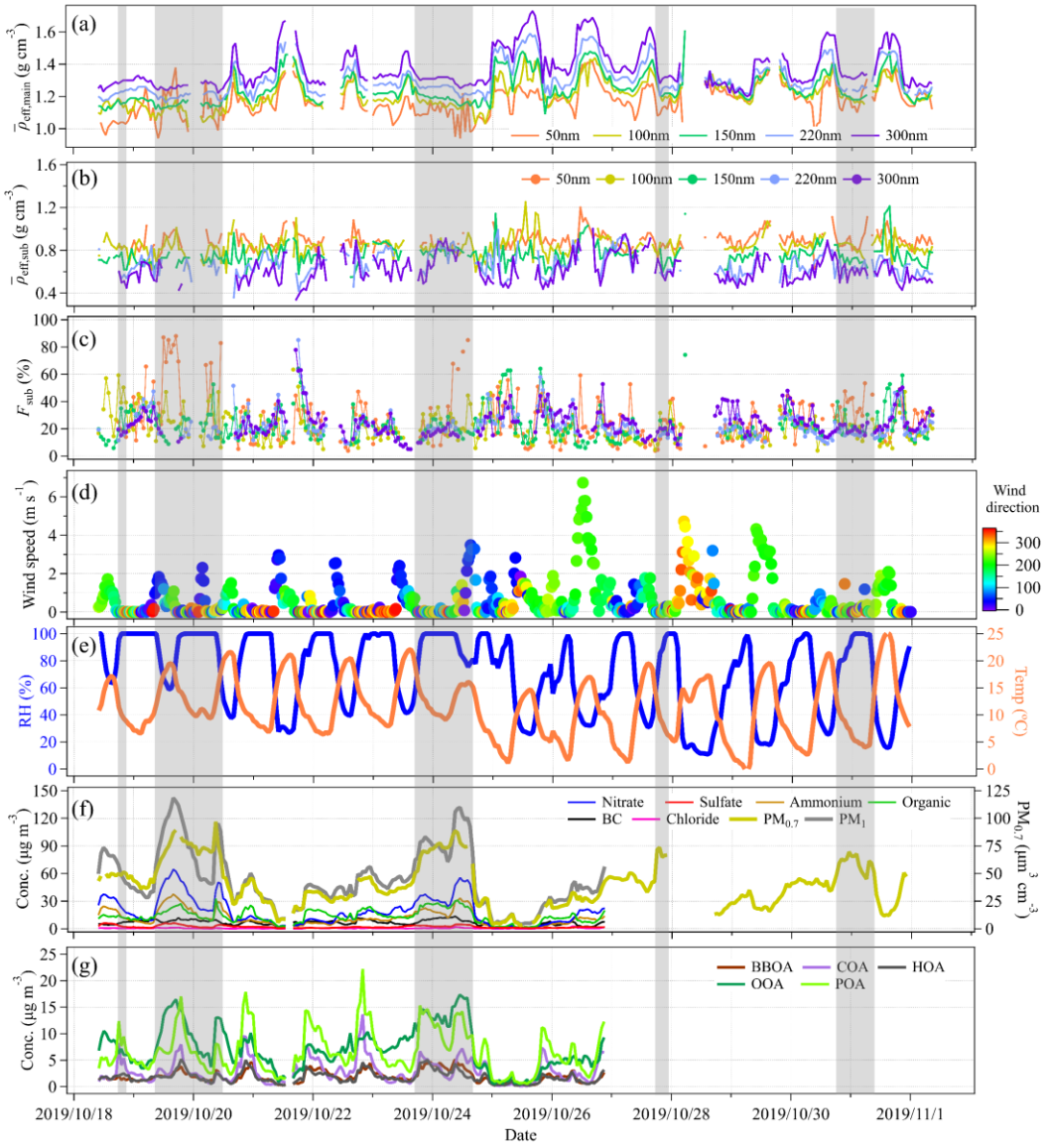

Figure R1 (S2). Timeseries of (a) geometric mean of the main-density mode ($\bar{\rho}_{eff,main}$), (b) geometric mean of the sub-density mode ($\bar{\rho}_{eff,sub}$), (c) number fraction of the sub-density mode (F_{sub}), (d) wind speed and wind direction, (e) relative humidity and temperature, (f) mass concentration of PM_1 chemical composition and (g) mass concentration of OA sources. The grey shaded areas represent the more polluted periods ($PM_{0.7}$ > 50 μm^3 cm^{-3}).

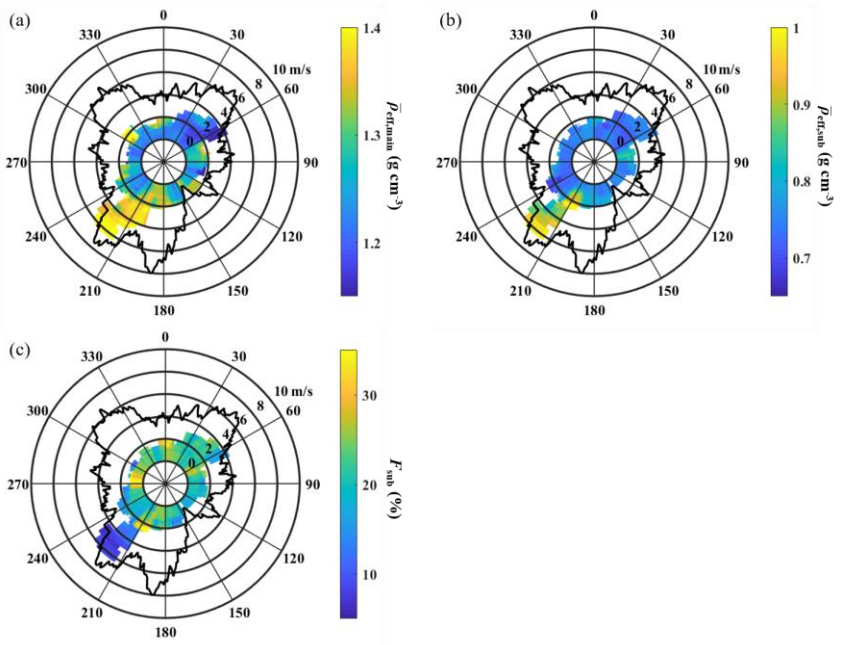

Figure R2 (3). Wind rose analysis of (a) geometric mean of the main-density mode ($\bar{\rho}_{\mathrm{eff,main}}$), (b) geometric mean of the sub-density mode ($\bar{\rho}_{\mathrm{eff,sub}}$), (c) number fraction of the sub-density mode (F_{sub}) for 150 nm particles. Black bold lines represent wind frequency during the entire sampling period.

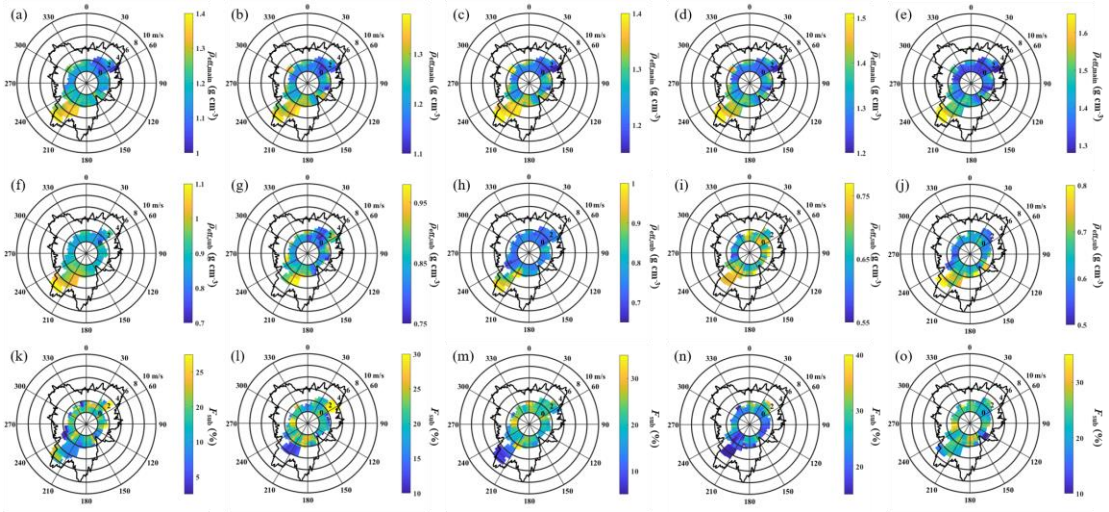

Figure R3 (S10). Wind rose analysis of (a)-(e): geometric mean of the main-density mode ($\bar{\rho}_{\mathrm{eff,main}}$), (f)-(j): geometric mean of the sub-density mode ($\bar{\rho}_{\mathrm{eff,sub}}$), (k)-(o): number fraction of the sub-density mode (F_{sub}) for 50, 100, 150, 220 and 300 nm particles. Black bold lines represent wind frequency during the entire sampling period.

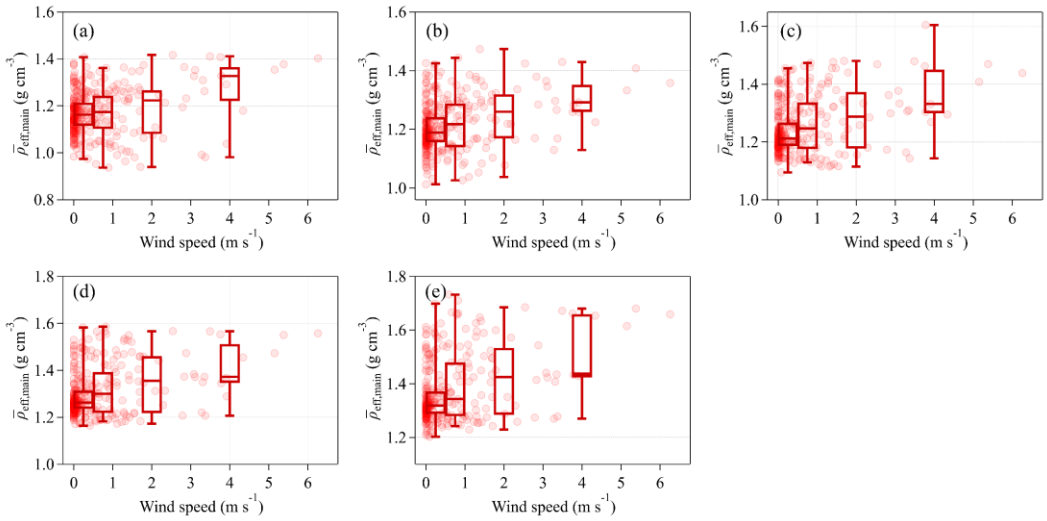

Figure R4 (S11). Box plots of geometric mean of the main-density mode ($\bar{\rho}_{eff,main}$) versus wind speed for (a) 50 nm, (b) 100 nm, (c) 150 nm, (d) 220 nm, and (e) 300 nm particles.

3. The authors mentioned some of the possible aerosol sources that can affect the aerosol measured in their site. I would like to see those on map (e.g. roads, factories, power plants). In addition, to study their role in the measured aerosol, I propose that the authors analyze wind directions (if available) and add discussion about it to the manuscript. E.g. quite recent studies for coal combustion emissions have reported effective densities >2 g/cm3 for particles, and it could be interesting to know if that kind of emission sources are near the measurement site possibly contributing to aerosol measured.

Response:

Following the reviewer's suggestion, we have added a map (Fig. S1) as well as detailed description in the text (Sect. 2.1) to elucidate the potential pollution sources within 5 km of sampling site: "*This site is located to the southwest of Beijing (~100 km) and northeast of Baoding, Hebei Province (~35 km). As shown in Fig. S1, the green area in the right panel is farmland and the faint yellow areas are scattered villages. The sampling site (red circle in Fig. S1) is surrounded by agricultural fields (mainly for corn cultivation) and is ~ 1.5 km away from the No.107 National Way. There is no significant emission sources such as large factories and power plants within 20 km. The main anthropogenic sources are biomass and coal combustion for domestic heating and cooking, as well as traffic in the country roads connecting villages. It should be noted that the heating season in China normally starts from 15 November to 15 March of the following year, which is not covered by our sampling period. Besides, the temperature during the measurement period varies from 0 to 25 °C (Fig. S2). The emission from heating is therefore considered to be limited. Moreover, source apportionment results also imply that the sampling site is not significantly affected by coal combustion during the observation period (Fig. S2). As shown in Fig. S1, one of the prevailing winds at the site is from southwest with relatively high wind speed, possibly indicating the influence of regional transport from southern Hebei Province. Overall, the sampling site is influenced by both local emissions from nearby villages and regional transport,*

and can well represent the average pollution condition of the rural area in the North China Plain (NCP) (Li et al., 2021a)."

We also added discussion about the influence of wind direction and wind speed on the pollution levels and particle effective density at the sampling site in Sect. 3.2 (see details in the reply to Comment #2). The influence of the traffic emissions from No.107 National Way is also discussed specifically in the text as: "*It is worth mentioning that* $\bar{\rho}_{eff,main}$ *and* $\bar{\rho}_{eff,sub}$ *do not show any obvious difference for wind direction of northwest. This implies that the influence of the traffic emission at No.107 National Way, which is approximate 1.5 km away from the sampling site (Fig. S1), on our measurements is somehow limited.*"

As discussed above, source apportionment results imply that the sampling site is not significantly affected by coal combustion during the observation. Therefore, the extremely high-density particles originated from coal combustion may not have much impact in our study.

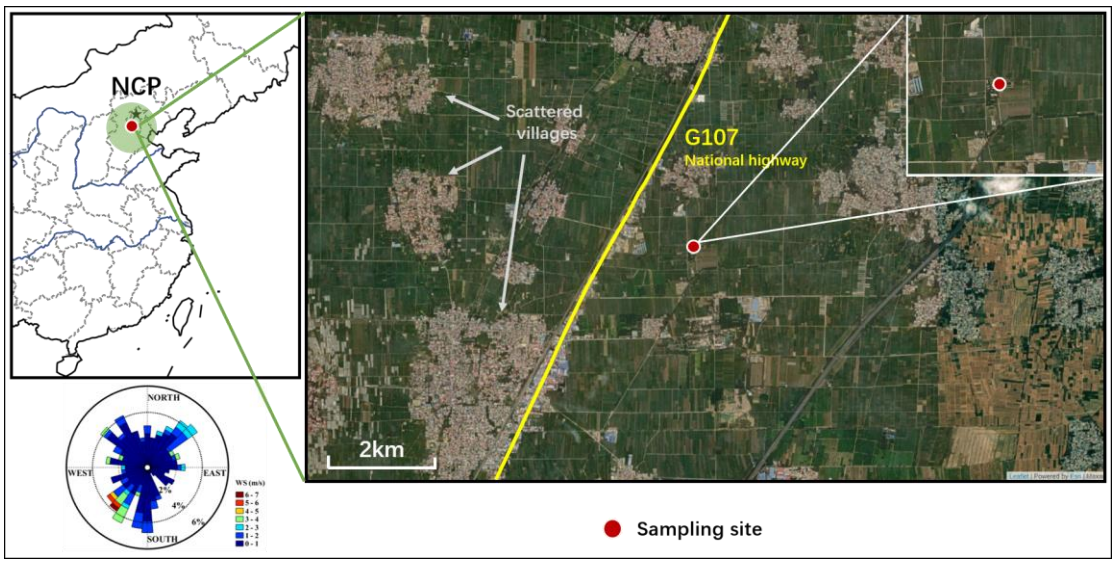

Figure R5 (S1). Location of the sampling site (marked in red circle) and statistic of wind frequency (the left-bottom of the figure). Satellite view from © ESRI.

4. In the experiment descriptions the authors write that they measured particle number size distributions also. It is not presented and analyzed in the manuscript. Why so? Could it be included into the analyses of size-resolved densities? In some previous studies made using SMPS-ELPI method the different densities have been connected to modes in particle number size distribution. It could be interesting and also important to see if this kind of results can be drawn from these experiments also.

Response:

Thanks for the suggestion. We agree with the reviewer that particle number distribution modes can reflect the sources and processes of the aerosol particles and may be connected to the variation of particle effective densities. Following the referee's suggestion, we tried to analyze the connections between the measured particle number size distribution and the effective density, and added the following discussion in Sect. 3.1: "*Interestingly, when we classify the measured particle number size distribution*

according to the measured F_{sub} and use the 25th and 75th percentiles of F_{sub} at each measured particle size as threshold, we found a more prominent Aitken mode with higher F_{sub} (F_{sub} > 75th F_{sub}) (Fig. S8). The initial burst of Aitken mode particles may be attributable to the enhanced traffic related emissions (Xie et al., 2017). Previous studies showed that the effective density of 50 nm traffic-emitted particles could be below 1.0 g cm^{-3} (Olfert et al., 2007; Park et al., 2003; Momenimovahed and Olfert, 2015). Therefore, the observed higher Aitken mode in our study may stem from the higher contribution of traffic emission, and subsequently lead to an increase of particles in the sub-density mode. This finding also provides a good support for the connections between F_{sub} and fresh emission sources."

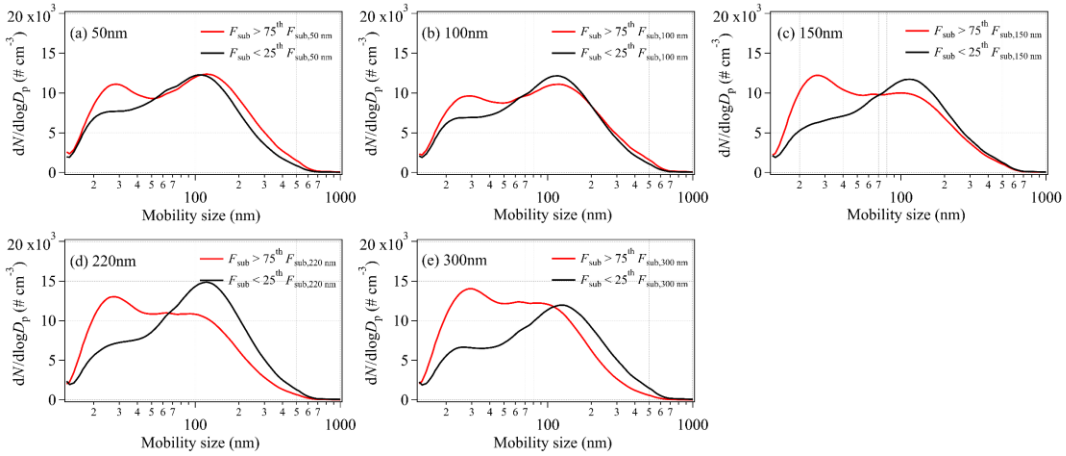

Figure R6 (S8). Particle number size distribution with high F_{sub} (F_{sub} > 75th F_{sub}) and low F_{sub} (F_{sub} < 25th F_{sub}) values for (a) 50 nm, (b) 100 nm, (c) 150 nm, (d) 220 nm, and (e) 300 nm particles.

5. The effective density of the particles can be affected by sampling method and treatment of the aerosol before the actual measurement. I would like short discussion in the manuscript regarding how the sampling and treatment used in this study possibly influence on the particle measured.

Response:

Following the reviewer's suggestion, we have added the discussion of the influence from the pre-sampling including drying before sampling and particle losses in the sampling tube in Sect. 2.1: "*There could be some possible influences from the pre-sampling treatment of ambient aerosols. One is the drying process in the sampling line since the evaporation of particle water content may affect its morphology. To date, only a few studies have investigated the influence of drying process on the particle effective density. Pagels et al. (2009) found that the influence of drying from RH of 80 % to 5 % could be negligible for 150 nm soot particles coated with $(NH_4)_2SO_4$. Yuan et al. (2020) concluded that the effective density of 240 nm BC particles coated with NH_4NO_3 respectively decreased by 5 % and 16 % for thickly and thinly coated particles when dry the particles from RH of 70 % to 5 %. According to these studies, the influence of the drying process on our effective density measurement is assumed to be negligible. Another possible influencing factor is the particle losses in the sampling line. Particles*

with size ranging from 50 to 500 nm, however, are not very sensitive to the three main loss mechanisms (i.e., diffusion loss, sedimentation loss and impaction loss) (Baron and Willeke, 2001). Furthermore, particle losses mainly affect the absolute particle number concentration. Its influence on the measurement of particle effective density is therefore considered to be negligible."

6. In the manuscript, the data have been divided to "polluted" and "clean" based on the PM0.7 results. How this PM0.7 was measured? Why these two were defined again in Figure 7 but now based on PM1 and with different threshold value? If PM0.7 is based on SMPS measurements, what are the limitation regarding that (e.g. knowledge of fractal dimension)? And in my opinion, the data labeled as "clean" is not very clean air, and I propose using "less polluted" and "more polluted" instead of current terms. Furthermore, it would be interesting to know how these less polluted and more polluted periods exist in timeline of the campaign. Are they from diurnal variation of concentrations or from changes in general pollution level?

Response:

Thanks for the comment. Following the reviewer's suggestion, we used "more polluted" and "less polluted" instead of original terms in the revised manuscript. Also, we have marked the "more polluted" periods by grey shades in Fig. R1 (Fig. S2). As can be seen in Fig. R1, the more polluted periods are mainly from the changes in general pollution level rather than diurnal variation of concentrations.

$PM_{0.7}$ is defined in our study as the total volume concentration of the particles in the size range of 13-700 nm calculated based on the PNSD measured by SMPS, while PM_1 is estimated based on ACSM measurement. ACSM data is only available between 18 October and 27 October, shorter than the effective density and PNSD data (covering from 18 October to 1 November). To better classify the pollution levels and avoid confusion, we now use $PM_{0.7}$ instead of PM_1 throughout the manuscript to divide our dataset into "more polluted" and "less polluted". In the calculation of $PM_{0.7}$, particles are assumed to be spherical (i.e., fractal dimension = 3), which may cause an underestimate of the volume concentration. But we think this may not affect the classification of pollution conditions in our study.

Accordingly, we have revised the text in Sect. 3.3 to describe the $PM_{0.7}$ threshold used in the classification as well as the relationship between $PM_{0.7}$ and PM_1 as: "*Given that the particle effective density varies dramatically with time (Fig. S9), the entire sampling period is classified into two pollution levels to elucidate the evolution of effective density under different pollution conditions. As mentioned in Sect. 2.1, particle mass concentration data only covers a part of the sampling period, and thus $PM_{0.7}$ volume concentration calculated based on SMPS measurement (size range of 13-700 nm) is applied to separate the sampling period into two groups: a more polluted group with $PM_{0.7}$ volume concentration higher than 50 μm^3 cm^{-3}, and a less polluted group corresponding to $PM_{0.7}$ volume concentration lower than 50 μm^3 cm^{-3}. It should be mentioned that the threshold of $PM_{0.7}$ volume concentration is comparable to PM_1 mass concentration of 60 μg m^{-3} (R^2 = 0.97, slope = 0.84, Fig. S12). The difference mainly stems from the size truncation of SMPS, as well as the time-dependent and size-*

dependent variations of the particle effective density (Morawska et al., 1999). Since particles are assumed to be spherical (i.e., fractal dimension = 3.0) in the calculation of $PM_{0.7}$, the obtained $PM_{0.7}$ may be overestimated."

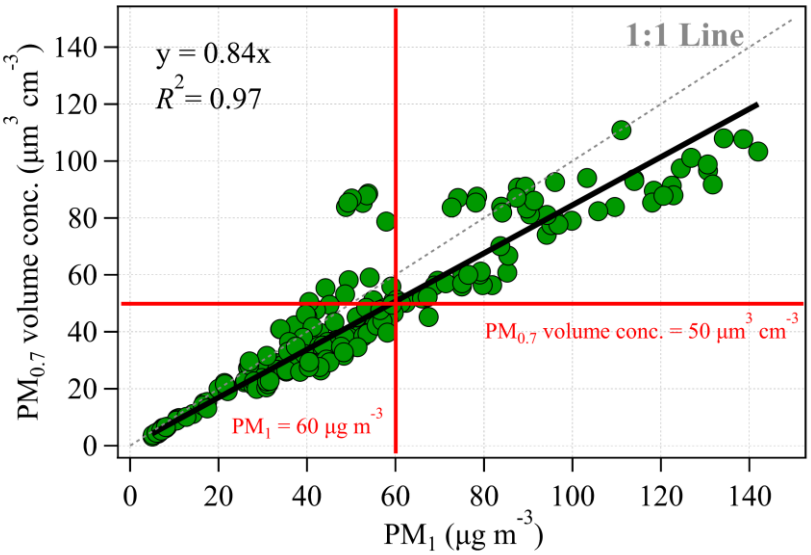

Figure R7 (S12). Comparison of $PM_{0.7}$ volume concentration and PM_1 mass concentration.

Technical questions and comments:

1. There are no clear descriptions of the meaning of colour code used in figure S3. In addition, the units for the colour axes are needed (#/cm3?).

Response:

Added as the reviewer suggested (Fig. S3 in the original SI has been changed to Fig. S9 in the revised SI).

2. Why the colours changed from fig 1 (main density mode indicated by blue) to fig 2 (main density mode indicated by black) and to fig 3 (main density mode indicated by red)? In general, please check the uniformity of the article (text, definitions, figures)

Response:

Changed as suggest. The colors for the main and sub-density mode in Fig. 1, Fig. 2 and Fig. 3 has been unified. We also went through the manuscript and made corrections to each part of the article including text, definitions, figures.

3. line 51: exits -> exist

Response:

Corrected.

Finally, thank you for the study which was made experimentally very well and which offered new insights to the characteristics of ambient aerosol. I hope that this kind of studies are made in future also in urban environments as well as directly for emission sources so that the whole picture of aerosols affecting our health and climate can be understood better.

Response:
Thanks for your supportive feedback.